Leaf Area Index Estimation Using Vegetation Indices Derived From Airborne Hyperspectral Images in Winter Wheat

Qiaoyun Xie, Wenjiang Huang, Dong Liang, Pengfei Chen, Chaoyang Wu, Guijun Yang, Jingcheng Zhang, Linsheng Huang, and Dongyan Zhang

***Abstract*—Continuous monitoring leaf area index (LAI) of field crops in a growing season has a great challenge. The development of remote sensing technology provides a good tool for timely mapping LAI regionally. In this study, hyperspectral reflectance data (405–835 nm) obtained from an airborne hyperspectral imager (Pushbroom Hyperspectral Imager) were used to model LAI of winter wheat canopy in the 2002 crop growing season. LAI was modeled based on its semi-empirical relationships with six vegetation indices (VIs), including ratio vegetation index (RVI), modified simple ratio index (MSR), normalized difference vegetation index (NDVI), a newly proposed index NDVI-like (which resembles NDVI), modified triangular vegetation index (MTVI2), and modified soil adjusted vegetation index (MSAVI). To assess the performance of these VIs, root mean square errors (RMSEs) and determination coefficient (R^2) between estimated LAI and measured LAI were reported. Our result showed that NDVI-like was the most accurate predictor of LAI. The inclusion of a green band in MTVI2 trended to give a rise to a much quicker saturation with increase of LAI (e.g., over 3.5). MSAVI and MTVI2 showed comparable but lower potential than NDVI-like in estimating LAI. RVI and MSR demonstrated their lowest prediction accuracy, implying that they are more likely to be affected by environmental conditions such as atmosphere and cloud, thus cannot properly reflect the properties of winter wheat canopy. Our results support the use of VIs for a quick assessment of seasonal variations in winter wheat LAI. Among the indices we tested in this study, the newly developed NDVI-like model created the most accurate and reliable results.**

***Index Terms*—Hyperspectral remote sensing, leaf area index (LAI), vegetation index (VI), winter wheat.**

Manuscript received February 16, 2014; revised June 04, 2014; accepted July 12, 2014. This work was supported in part by the Hundred Talent Program of the Chinese Academy of Sciences of W. Huang and in part by the National Natural Science Foundation of China under Grant 41271412 and Grant 41301471.

Q. Xie and W. Huang are with the Key Laboratory of Digital Earth Science, Institute of Remote Sensing and Digital Earth, Chinese Academy of Sciences, Beijing 100094, China (e-mail: xieqiaoyun2011@gmail.com; huangwenjiang@gmail.com).

D. Liang, L. Huang, and D. Zhang are with the Key Laboratory of Intelligent Computer and Signal Processing, Ministry of Education, Anhui University, Hefei 230039, China (e-mail: dliang@ahu.edu.cn; linsheng0808@163.com; hello-lion@hotmail.com).

P. Chen is with the State Key Laboratory of Resources and Environment Information System, Institute of Geographic Science and Natural Resources Research of Chinese Academy of Sciences, Beijing 100101, China (e-mail: pengfeichen@igsnrr.ac.cn).

C. Wu is with the State Key Laboratory of Remote Sensing Science, Institute of Remote Sensing and Digital Earth, Chinese Academy of Sciences, Beijing 100101, China (e-mail: hefery@163.com).

G. Yang and J. Zhang are with the Beijing Research Center for Information Technology in Agriculture, Beijing 100097, China (e-mail: guijun.yang@163.com; zhangjc@nercita.org.cn).

Color versions of one or more of the figures in this paper are available online at http://ieeexplore.ieee.org.

Digital Object Identifier 10.1109/JSTARS.2014.2342291

I. Introduction

LEAF AREA INDEX (LAI) describes a potential surface area available for leaf gas exchange between the atmosphere and the terrestrial biosphere, and it determines the transpiration, the interception and absorption rates by vegetation in solar radiation [1]. Therefore, it is a crucial input variable in numerous land surface models and is one of the most important agronomic indices to monitor crop condition and estimate yield. Traditional determination of LAI involves direct field measurement, which is time-consuming and labor-intensive, making it hard to be applied in a large area and long-term monitoring. In comparison, remote sensing technology provides a good and reliable approach for timely evaluation of LAI at a large scale [2].

Many physical and statistical models have been developed to estimate LAI using optical remote sensing data. Using a physical model, a three-dimensional radiative transfer model has been inverted to retrieve global LAI products of Moderate-Resolution Imaging Spectroradiometer (MODIS) data using a lookup table [3]. Neural network is also developed to generate canopy biophysical products from top-of-canopy reflectance measurements [4], [5]. Although these techniques have been widely used to estimate LAI at large scales, studies also show that the accuracy of these models may not meet specific application requirements in certain cases [6].

Statistical models generally use regression methods between spectral variables and measured LAI [7]. The principal component analysis is one of such approaches, in which LAI is estimated from a set of features transformed from the original radiometric measurements [8]. Although this approach incorporates information of all spectral bands, it is not a straightforward interpretation to the physical meaning of the extracted features. In contrast, spectral vegetation indices (VIs) combining reflectance from a few spectral bands and being relatively simple have been related with various biophysical descriptors and used for estimating LAI of different crops [9].

TABLE I
DESCRIPTIONS OF EXPERIMENTAL DESIGN OF WINTER WHEAT

W / M^3 HA^{-1}	N / KG HA^{-1}											
	0			150			300			450		
0	12	11	10	9	8	7	6	5	4	3	2	1
225	13	14	15	16	17	18	19	20	21	22	23	24
450	36	35	34	33	32	31	30	29	28	27	26	25
675	37	38	39	40	41	42	43	44	45	46	47	48
SPECIES	9507	9428	JD 8	9507	9428	JD 8	9507	9428	JD 8	9507	9428	JD 8

N stands for nitrogen, W stands for water, and JD 8 stands for Jingdong 8.

Broadband indices are heavily affected by soil background at a low vegetation cover. The advent of airborne hyperspectral image has made it possible to construct more refined VIs through the use of distinct narrow bands [10]. VIs have been applied in cases of different crops [11]–[14]. However, most VIs are species specific and are not robust when used across different species [15]. The main objective of this study is to compare the potential of different VIs derived from airborne hyperspectral reflectance in predicting LAI of winter wheat over growing seasons. Six types of VIs were used in this analysis: 1) ratio vegetation index (RVI) [16], 2) modified simple ratio index (MSR) [16], 3) normalized difference vegetation index (NDVI) [17], 4) NDVI-like [18], 5) modified triangular vegetation index (MTVI2) [9], and 6) modified soil adjusted vegetation index (MSAVI) [19]. RVI, MSR, and NDVI are normal and basic indices which are usually used as a baseline of VIs [12]. NDVI-like is a derivative of NDVI and is modified on the basis of NDVI. MTVI2 and MSAVI were chosen because they were proved sensitive to wheat [9], [20].

II. MATERIALS

A. Experimental Design

The experiment was conducted in the 2002 growing season at National Experimental Station for Precision Agriculture ($40°10'$N, $116°27'$E), Beijing, China [21]. Forty-eight fields each in a size of $32.4\,\mathrm{m} \times 30\,\mathrm{m}$ were selected for LAI sampling, and they were numbered 1 through 48 (the location of each plot can be seen in Table I). Three types of winter wheat (W 9507, W 9428, and W Jingdong 8) were planted in these fields. We also designed varieties of water irrigation and nitrogen fertilization in this experiment. There were overall four nitrogen treatments (0, 150, 300, and $450\,\mathrm{kg\,ha^{-1}}$) and four water treatments (0, 225, 450, and $675\,\mathrm{m^3\,ha^{-1}}$). Thereby, our test encompassed a combination of species, nitrogen, and water regimes (Table I).

B. Data Collection

1) Image Acquisition and Preprocessing: Pushbroom Hyperspectral Imager (PHI) is an array pushing imaging spectrometer designed by Shanghai Institute of Technical Physics, the Chinese Academy of Sciences, with a spectral resolution less than 5 nm, spanning wavelengths from 405 to 835 nm with 126 bands. During the 2002 growing season, three flights were taken on April 18, May 17, and May 31, respectively. The flying heights varied between 1000 and 1200 m and the fight path consisted of seven strips, covering the whole station (i.e., National Experimental Station for Precision Agriculture). The spatial resolution of corrected PHI images was 1 m. Apart from a regular atmospheric correction, with a normally used filtering method: Savitzky-Golay, the three flights of PHI images were denoised to further improve the image quality [22].

2) LAI Data: In each field, LAIs were sampled and recorded in three times on April 18, May 17, and May 31, respectively (so, a total of $48 \times 3 = 144$). LAI sampling was performed within a $1 \times 1\,\mathrm{m}^2$ plot in a field (i.e., in three different locations for each field). Wheat leaf samples were collected in each plot, and their location was recorded using a GPS equipment (Trimble DSM 232 DGPS) with an accuracy of 0.2 m. The GPS measurements could help locate an LAI sampling plot on a PHI image. The leaf areas of winter wheat were measured in a laboratory to determine LAI. After eliminating four invalid samples on May 31 because of their values equal zero, the final dataset contained 140 samples. From LAI sampling plots on the PHI images acquired on the three different dates, corresponding image spectra were extracted in order to conduct modeling analyses with measured LAIs below.

III. METHODS

A. Vegetation Indices

NDVI highlights the striking contrast between near-infrared (NIR) and red band reflectance. Although some studies point out that NDVI is not the best approach for LAI estimation because the inherent saturation drawback hinders effective estimation of LAI, it has been widely accepted by both research and social application communities as a benchmark for comparing alternative inversion algorithms [9]. RVI can compress the multiplicative effects of atmosphere and has a close linear relationship with biological parameters of plants [12]. MSR aims at alleviating the saturation drawback of NDVI. Broge and Leblanc [23] found that the MSAVI was the best LAI estimator for its lowest sensitivity to soil effects on canopy spectrum and soil spectral properties. One particular limitation of MSAVI was its performance as an estimator of LAI in dense canopies. Modified MTVI2 was

TABLE II
DEFINITIONS AND FORMULAS OF VIs INVESTIGATED IN THIS STUDY

Index	Abbr.	Formula	Reference	Bands applied
Ratio vegetation index	RVI	$RVI = \rho_{nir} / \rho_{red}$	[16]	660 nm 785 nm
Modified simple ratio index	MSR	$MSR = \frac{\rho_{nir} / \rho_{red} - 1}{\sqrt{\rho_{nir} / \rho_{red} + 1}}$	[16]	660 nm 785 nm
Normalized difference vegetation index	NDVI	$NDVI = \frac{\rho_{nir} - \rho_{red}}{\rho_{nir} + \rho_{red}}$	[17]	660 nm 785 nm
NDVI-like	NDVI -like	$NDVI = \frac{\rho_1 - \rho_2}{\rho_1 + \rho_2}$	[18]	700 nm 724 nm
Modified triangular vegetation index	MTVI2	$MTVI2 = \frac{1.5*(1.2*(\rho_{nir} - \rho_{green}) - 2.5*(\rho_{red} - \rho_{green}))}{\sqrt{(2*\rho_{nir}+1)^2 - (6*\rho_{nir} - 5*\sqrt{\rho_{red}}) - 0.5}}$	[9]	576 nm 660 nm 785 nm
Modified soil-adjusted vegetation index	MSAVI	$MASVI = \frac{2*\rho_{nir} + 1 - \sqrt{(2*\rho_{nir}+1)^2 - 8*(\rho_{nir} - \rho_{red})}}{2}$	[17]	660 nm 785 nm

first developed by Haboudane *et al*. [16]. It combines hyperspectral reflectance in NIR, red and green wavelengths to reduce perturbation from leaf chlorophyll content variation for crop green LAI estimation, and incorporates an adjustment mechanism to reduce background soil effect. In fact, MTVI2 was especially developed for hyperspectral data. Liu *et al*. [9] have proved that MTVI2 was quite promising in crop LAI estimation and could be used in a simple regression model to generate a baseline green LAI product for seasonal crop growth monitoring. Table II lists all six VIs including their definitions and references.

Apart from those VIs aforementioned, many researchers are interested in developing many other VIs with hyperspectral data [10]. For example, Darvishzadeh *et al*. [18] developed a new index called NDVI-like based on red and NIR bands, and showed strong ability to estimate LAI of grassland. To verify those indices, it is necessary to assess the performance of these two-band indices in estimating winter wheat LAI by comparing them with traditional indices. Development of ground hyperspectral remote sensing and imaging spectrometry has opened new channels for monitoring plant growth and estimating biophysical properties of vegetation. A new group of VIs based on the shape and relative position of the spectral reflectance curve has been proposed, among which NDVI-like is an inspiring one.

Regression models based on VIs are widely used for estimating biophysical parameters due to high computation efficiency and universality. In order to evaluate hyperspectral VIs for estimating LAI, in this study, a regression analysis was conducted between LAI and various VIs, including MSR, RVI, NDVI, MSAVI, and MTVI2, and a newly proposed index NDVI-like. The narrow band NDVI-like index was systematically calculated for all possible 126 × 126 = 15 876 wavelength combinations between 405 and 835 nm. We calculated all possible combinations of 126 hyperspectral bands using MATLAB. Correlation analysis was performed between 140 LAI samples and their corresponding NDVI-like combinations.

B. Validation of Statistical Techniques

To evaluate the performance of the statistical models, a k-fold cross-validation procedure was used, in which the entire dataset (i.e., 140 samples) acquired in 2002 was divided into k mutually exclusive groups following a k-fold cross-validation partitioning design. In our case, the data was randomly and evenly split into four ($k = 4$) sets, and each quarter was estimated by the remaining samples. In other words, for estimating LAI with one type of VI, we developed four individual models in rotating one quarter as validation data. In each model, 105 samples were used to build the calibration model, and the remaining 35 samples were used to verify the calibration model. All six VIs tested used the same k-fold partitions.

This type of validation was necessary because it reduced the dependence on a single random partition into calibration and validation datasets. This also guaranteed that all samples were used for both training and validation with each sample used for validation exactly once. root mean square errors (RMSEs) and determination coefficient (R^2) were selected as the accuracy indicators of the statistical models in predicting unknown samples [24].

IV. RESULTS AND DISCUSSION

A. Calibration and Validation of Models

Per each of the six VIs, we developed four individual models. Since all tested VIs used the same k-fold partitions, the results of different indices were comparable. In order

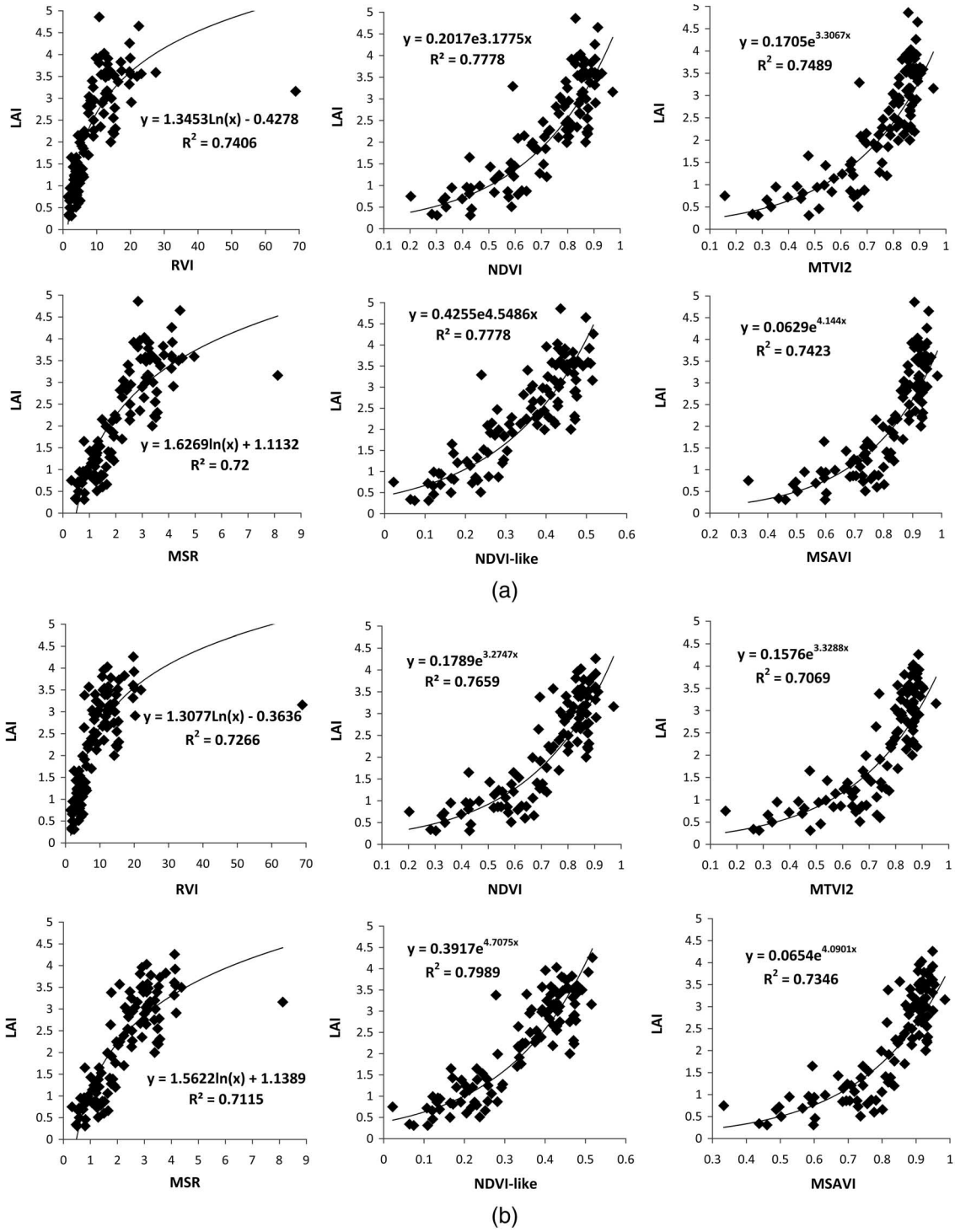

Fig. 1. Calibration of models in four groups: (a) Group 1; (b) Group 2; (c) Group 3; and (d) Group 4.

to facilitate a comparison of these indices, we divided the calibration models into four groups, each group with the same observation dataset. The calibration models are presented in Fig. 1. From this figure, among the tested VIs, NDVI-like exhibited the best R^2, followed by NDVI and then others. Judged by the fit lines, the RVI and MSR calibration models were of all logarithm models, meanwhile the other VIs were exponential models, except for one linear model of NDVI-like in Group 3. Among these models, scattering points in RVI and MSR models exhibited a higher scattered degree along the best fit line than other VIs, especially when LAI value was greater than 3. In Groups 1, 2, and 3, there was one point in each RVI and MSR model that far deviated from the fit line, suggesting the limitation of ratio index in LAI prediction.

The saturation effect was studied under a visual comparison. Fig. 1 shows that the saturation is not only a constraint of

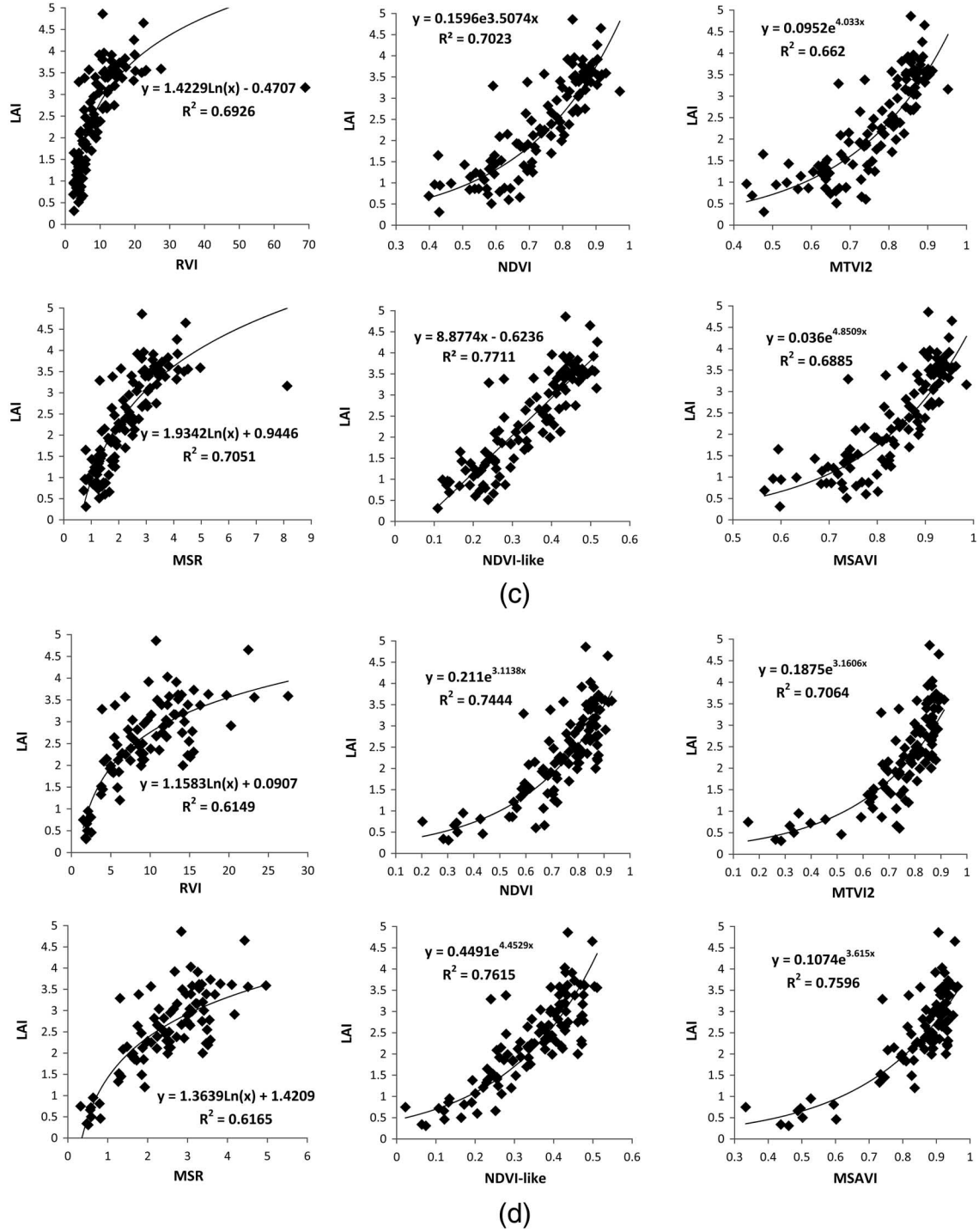

Fig. 1. *(Continued.)*

NDVI method, MTVI2 and MSAVI models also have this type of problem, especially in Groups 1, 2, and 4. The NDVI-like model was superior to NDVI model in every group and created the highest R^2 (0.80) at band 77 (700 nm) and band 83 (724 nm), supporting the study by Darvishzadeh *et al*. [18].

Table III presents the determination coefficient (R^2) of each calibration model. In each column for each type of VI, R^2 varies from Group 1 through Group 4. RVI models created a widest range of R^2variation (from 0.6149 to 0.7406), second by MSR (from 0.6165 to 0.7200), then MTVI2 (from 0.6620 to 0.7489), and NDVI (from 0.7023 to 0.7778), MSAVI (from 0.6885 to 0.7596), and NDVI-like (from 0.7615 to 0.7989). We can conclude that NDVI-like is the most robust type of VI. In each row for each group, NDVI-like showed relatively higher R^2 value than other VIs, therefore it was the most accurate VI.

B. Evaluation of VIs

LAI predicted by developed models were compared to measured LAI values using six types of VIs. For each VI,

TABLE III
DETERMINATION COEFFICIENT (R^2) OF EACH CALIBRATION MODEL

Group	VI					
	RVI	MSR	NDVI	NDVI-like	MTVI2	MSAVI
Group 1	0.7406	0.7200	0.7778	0.7778	0.7489	0.7423
Group 2	0.7266	0.7115	0.7659	0.7989	0.7069	0.7346
Group 3	0.6926	0.7051	0.7023	0.7711	0.6620	0.6885
Group 4	0.6149	0.6165	0.7444	0.7615	0.7064	0.7596

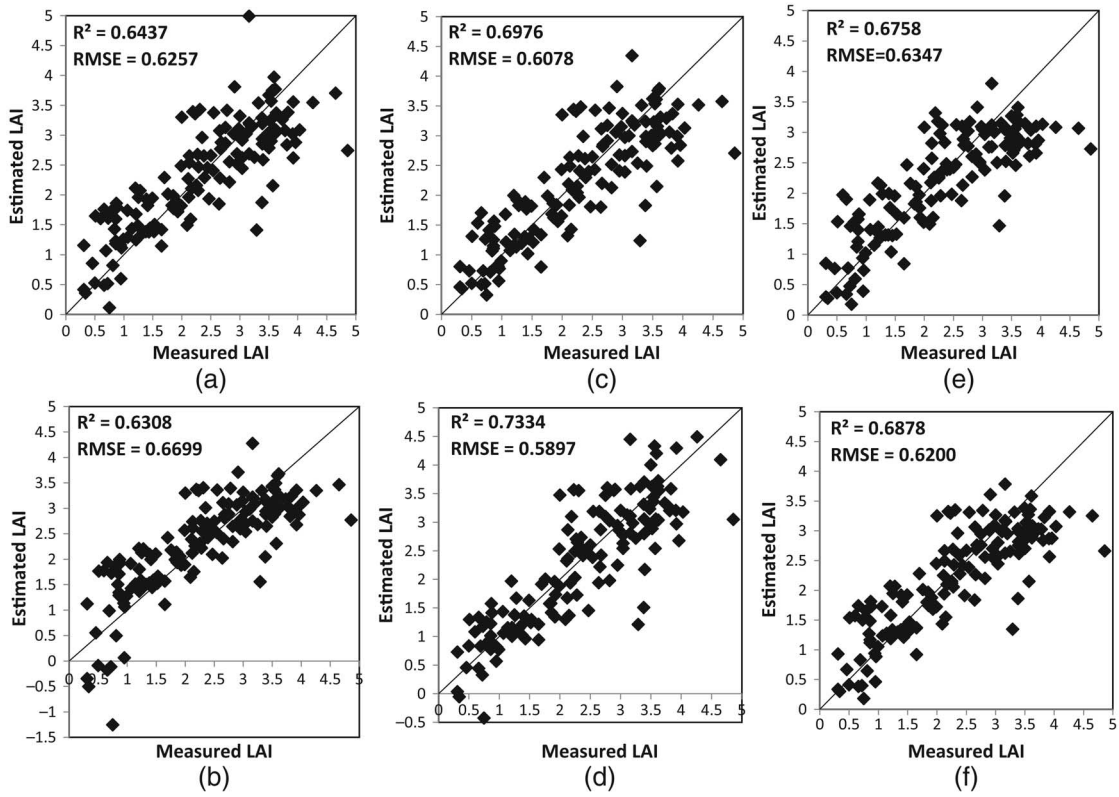

Fig. 2. Relationship between measured LAI and estimated LAI using six types of VIs: (a) RVI; (b) MSR; (c) NDVI; (d) NDVI-like; (e) MTVI2; and (f) MSAVI.

predicted samples in Group 1 through Group 4 were validated together (35 predicted samples in each group, and 140 in total). The confidence of the relationship was assessed by the RMSE and R^2 values (Fig. 2).

Our results evidently showed that NDVI-like well made LAI estimates. When the measured LAI was greater than a threshold (about 3.5–4), all estimated LAI values were lower than the ground LAI values, except some using the NDVI-like model. When measured LAI was greater than 3.5, the estimated LAI values using the NDVI-like model were slightly higher than measured LAI values, suggesting the powerful prediction ability of the NDVI-like index. In addition, among the six VIs in Fig. 2, NDVI-like samples best converged to the 1:1 line. The R^2 for all VIs varied between 0.6308 and 0.7334, and meanwhile the RMSE varied between 0.5897 and 0.6699. The best index using all samples was NDVI-like ($R^2 = 0.7334$, $\mathrm{RMSE} = 0.5897$), followed by NDVI ($R^2 = 0.6976$, $\mathrm{RMSE} = 0.6078$), then MSAVI ($R^2 = 0.6878$, $\mathrm{RMSE} = 0.62$), and MTVI2 ($R^2 = 0.6758$, $\mathrm{RMSE} = 0.6347$). RVI and MSR demonstrated the lowest prediction accuracy, implying that the construction of these indices did not reflect leaf optical properties and canopy structure properly.

Based on the LAI estimate results addressed above, it is clear that the NDVI-like has demonstrated its potential to estimating winter wheat LAI. First, NDVI-like has already clearly showed its performance from our research results. In addition, in this study, NDVI-like was based on red (700 nm) and red edge (724 nm) bands. Red edge optical parameters are relatively insensitive to environment changes such as soil cover percentage, atmospheric effects, canopy structure, and solar zenith angle [25], so it is useful for LAI estimation.

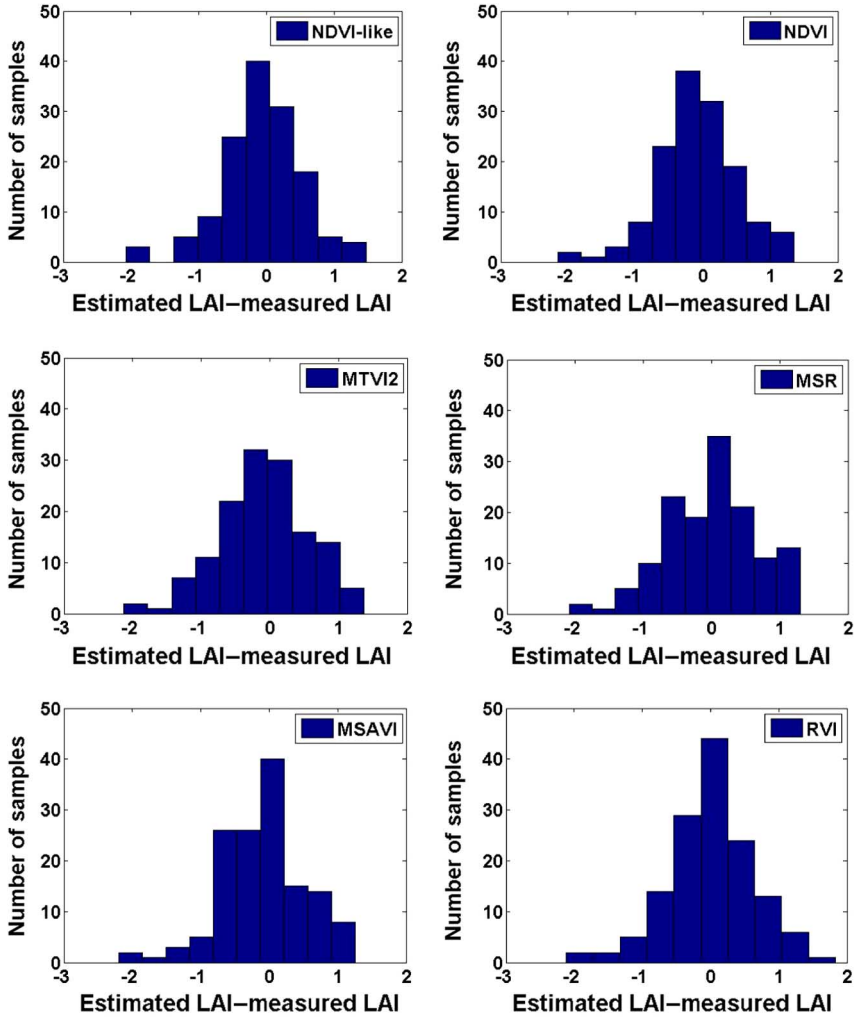

Fig. 3. Statistical distribution of the difference between the estimated LAI and measured LAI using the six VIs.

Furthermore, Fig. 3 shows the distribution of the difference between the measured LAI and estimated LAI values for all the validation samples in all models of the six VIs (35 predicted samples in each group, and 140 in total). We defined "error" here as a value of estimated LAI minus measured LAI. RVI and NDVI-like errors best submit a normal distribution, and NDVI-like error figure is more clustered around zero, implying a higher accuracy. It is apparent that NDVI-like is the most accurate index for the LAI estimation. MSAVI did not create higher R^2 than NDVI-like and NDVI. This might be because soil background was not very complex, i.e., dry, bright, and similar soil background among the 140 LAI measurement plots [10]. In terms of MTVI2, the agreement between the estimated and the measured LAI was relatively poor when measured LAI was greater than 3. This was not consistent with the work done by Haboudane *et al*. [16], which concluded that MTVI2 was sensitive to high LAI. However, the result was consistent with the conclusion made by Liu *et al*. [9], in which MTVI2's ability to estimate crop LAI was weaker for wheat than for other species. The low R^2 values of RVI and MSR suggested that these two indices were easy to be affected by environmental conditions such as atmosphere and cloud, even though the soil background was relatively simple. Consequently they could not properly reflect the properties of winter wheat canopy. NDVI and NDVI-like demonstrated a stable ability in winter wheat LAI estimation, especially NDVI-like, based on red and NIR or red-edge bands. These bands are related to plant leaf water content that has a close correlation with canopy biomass and LAI and an indirect correlation to the absorption features of protein, nitrogen, lignin, cellulose, and starch concentrations [10]. The two bands selected to calculate NDVI-like maximized the correlation between LAI and NDVI-like, thus best captured the spectral characteristics of winter wheat canopy and created the highest estimation accuracy.

V. Conclusion

The results of the study demonstrated that winter wheat LAI could be estimated through the inversion of vegetation index models with a satisfactory accuracy. Strong relationships were found between VIs and LAI based on reflectance in the red, NIR, red-edge, and green band. Based on red and NIR or red-edge bands, NDVI and NDVI-like provided better results

than RVI and MSR. MTVI2 enhanced the performance by including green band, while it was less satisfactory than NDVI and NDVI-like, especially when LAI values were greater than 3.5.

Among the six indices tested in this study, the newly developed index NDVI-like was found to be most closely related with LAI and thus exhibited the highest sensitivity to winter wheat LAI than other five widely used indices. This was consistent with the study of Darvishzadeh *et al*. [18]. It has a potential to be used in a simple regression model to generate baseline LAI of crops, and therefore it can be useful for seasonal growth monitoring of winter wheat. In this experiment, the results also indicated that other indices trended to saturate at higher LAI values (e.g., greater than 3.5).

ACKNOWLEDGMENT

We would like to acknowledge the field campaign at National Experimental Station for Precision Agriculture and the stuff there in the management of flight test and the crop planting. Many thanks to Y. Hu for helping with the image processing and IDL programming. Our appreciation also goes to the anonymous reviewers for valuable suggestions and comments.

REFERENCES

[1] J. Monteith and M. Unsworth, *Principles of Environmental Physics: Plants, Animals, and the Atmosphere*. New York, NY, USA: Academic, 2013.

[2] Y. Dong, *Analyzing Special Scale Problems of Crop Growth Parameters for Growth Monitoring With Multi-Scale Remote Sensing Data*. Hangzhou, China: School Res. Environ., Zhejiang Univ., 2013.

[3] Y. Knyazikhin *et al*., "Synergistic algorithm for estimating vegetation canopy leaf area index and fraction of absorbed photosynthetically active radiation from MODIS and MISR data," *J. Geophys. Res.: Atmos. (1984–2012)*, vol. 103, no. D24, pp. 32257–32275, 1998.

[4] C. Bacour, F. Baret, and D. Beal, "Neural network estimation of LAI, fAPAR, fCover and LAI, from top of canopy MERIS reflectance data: Principles and validation," *Remote Sens. Environ*., vol. 105, no. 4, pp. 313–325, 2006.

[5] F. Baret *et al*., "LAI, fAPAR and fCover CYCLOPES global products derived from VEGETATION: Part 1: Principles of the algorithm," *Remote Sens. Environ*., vol. 110, no. 3, pp. 275–286, 2007.

[6] F. Canisius, R. Fernandes, and J. Chen, "Comparison and evaluation of medium resolution imaging spectrometer leaf area index products across a range of land use," *Remote Sens. Environ*., vol. 114, no. 5, pp. 950–960, 2010.

[7] R. Fernandes *et al*., "Landsat-5 TM and Landsat-7 ETM+ based accuracy assessment of leaf area index products for Canada derived from SPOT-4 VEGETATION data," *Can. J. Remote Sens*., vol. 29, no. 2, pp. 241–258, 2003.

[8] R. Pu and P. Gong, "Wavelet transform applied to EO-1 hyperspectral data for forest LAI and crown closure mapping," *Remote Sens. Environ*., vol. 91, no. 2, pp. 212–224, 2004.

[9] J. Liu, E. Pattey, and J. Guillaume, "Assessment of vegetation indices for regional crop green LAI estimation from Landsat images over multiple growing seasons," *Remote Sens. Environ*., vol. 123, pp. 347–358, 2012.

[10] P. Gong *et al*., "Estimation of forest leaf area index using vegetation indices derived from Hyperion hyperspectral data," *IEEE Trans. Geosci. Remote Sens*., vol. 41, no. 6, pp. 1355–1362, Jun. 2003.

[11] E. Boegh *et al*., "Airborne multispectral data for quantifying leaf area index, nitrogen concentration, and photosynthetic efficiency in agriculture," *Remote Sens. Environ*., vol. 81, no. 2, pp. 179–193, 2002.

[12] N. H. Broge and J. V. Mortensen, "Deriving green crop area index and canopy chlorophyll density of winter wheat from spectral reflectance data," *Remote Sens. Environ*., vol. 81, no. 1, pp. 45–57, 2002.

[13] R. Colombo *et al*., "Retrieval of leaf area index in different vegetation types using high resolution satellite data," *Remote Sens. Environ*., vol. 86, no. 1, pp. 120–131, 2003.

[14] P. Curran, "Estimating green LAI [leaf area index] from multispectral aerial photography," *Photogramm. Eng. Remote Sens*., vol. 49, no. 12, pp. 1709–1720, 1983.

[15] A. Viña *et al*., "Comparison of different vegetation indices for the remote assessment of green leaf area index of crops," *Remote Sens. Environ*., vol. 115, no. 12, pp. 3468–3478, 2011.

[16] D. Haboudane *et al*., "Hyperspectral vegetation indices and novel algorithms for predicting green LAI of crop canopies: Modeling and validation in the context of precision agriculture," *Remote Sens. Environ*., vol. 90, no. 3, pp. 337–352, 2004.

[17] J. Rouse, Jr., *et al*., "Monitoring vegetation systems in the great plains with ERTS," *NASA Spec. Publ*., vol. 351, pp. 309, 1974.

[18] R. Darvishzadeh *et al*., "Mapping grassland leaf area index with airborne hyperspectral imagery: A comparison study of statistical approaches and inversion of radiative transfer models," *ISPRS J. Photogramm. Remote Sens*., vol. 66, no. 6, pp. 894–906, 2011.

[19] J. Qi *et al*., "A modified soil adjusted vegetation index," *Remote Sens. Environ*., vol. 48, no. 2, pp. 119–126, 1994.

[20] K. Huber *et al*., "Leaf area index determination of wheat indicating heterogeneous soil conditions," vol. 6359, pp. 63590M–63590M-9, 2006.

[21] W. Huang *et al*., "Identification of yellow rust in wheat using in-situ spectral reflectance measurements and airborne hyperspectral imaging," *Precis. Agric*., vol. 8, no. 4–5, pp. 187–197, 2007.

[22] S. Abraham and M. J. E. Golay, "Smoothing and differentiation of data by simplified least squares procedures," *Anal. Chem*., vol. 36, no. 8, pp. 1627–1639, 1964.

[23] N. H. Broge and E. Leblanc, "Comparing prediction power and stability of broadband and hyperspectral vegetation indices for estimation of green leaf area index and canopy chlorophyll density," *Remote Sens. Environ*., vol. 76, no. 2, pp. 156–172, 2001.

[24] C. Wu *et al*., "Predicting leaf area index in wheat using angular vegetation indices derived from in situ canopy measurements," *Can. J. Remote Sens*., vol. 36, no. 4, pp. 301–312, 2010.

[25] R. Pu *et al*., "Extraction of red edge optical parameters from Hyperion data for estimation of forest leaf area index," *IEEE Trans. Geosci. Remote Sens*., vol. 41, no. 4, pp. 916–921, Apr. 2003.

Qiaoyun Xie received the Master degree in signal and information processing from Anhui University, Hefei, China, in 2014. Currently, pursuing the Ph.D. degree in Key Laboratory of Digital Earth Science, Institute of Remote Sensing and Digital Earth, Chinese Academy of Sciences, Beijing, China.

Her research interests include quantitative remote sensing application in agriculture and development of software for digital image processing.

Wenjiang Huang received the Ph.D. degree in cartography and GIS from Beijing Normal University, Beijing, China, in 2005.

Currently, he is a Professor with the Key Laboratory of Digital Earth Science, Institute of Remote Sensing and Digital Earth, Chinese Academy of Sciences, Beijing, China. His research interests include quantitative remote sensing research and application in vegetation.

Dong Liang received the Ph.D. degree in circuits and systems from Anhui University, Hefei, China, in 2002.

Currently, he is a Professor with the Key Laboratory of Intelligent Computing and Signal Processing, Ministry of Education, Anhui University, Hefei, China. His research interests include image processing, computing signal processing, and pattern recognition.

Pengfei Chen received the M.S. degree in grass science and the Ph.D. degree in land use and information technology from China Agricultural University, Beijing, China, in 2006 and 2009, respectively.

From July 2009, he works with the Institute of Geographic Sciences and Natural Resources Research of Chinese Academy of Sciences, Beijing, China. Currently, he is an Assistant Researcher in this institute. His research interests include application of remote sensing and crop growth model technology in agricultural management.

Chaoyang Wu received the Ph.D. degree in cartography and geographic information systems from Chinese Academy of Sciences, Beijing, China, in 2010.

Currently, he is a Professor with the Institute of Remote Sensing and Digital Earth, Chinese Academy of Sciences, Beijing, China. His research interests include remote sensing of vegetation primary productivity, ecological modeling, and impacts of climate changes on carbon sequestration.

Guijun Yang received the Ph.D. degree in cartography and geographic information systems from the State Key Laboratory of Remote Sensing Science, Institute of Remote Sensing Applications, Chinese Academy of Sciences, Beijing, China, in 2008.

Currently, he is a Research Associate with the Beijing Research Center for Information Technology in Agriculture, Beijing, China. His research interests include radiative transfer modeling, imagery simulation, atmospheric correction, and quantitative inversion.

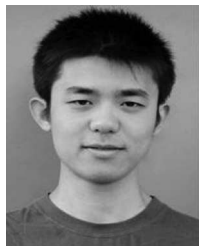

Jingcheng Zhang received the Ph.D. degree in agricultural remote sensing and information technology from Zhejiang University, Hangzhou, China, in 2012.

Currently, he is with the Beijing Research Center for Information Technology in Agriculture, Beijing, China. His research interests include hyperspectral analyzing, agricultural disease detection, and monitoring by incorporating multisources of remote sensing data.

Linsheng Huang received the Ph.D. degree in circuits and systems from Anhui University, Hefei, China, in 2013.

Currently, he is a lecturer with the Key Laboratory of Intelligent Computing and Signal Processing, Ministry of Education, Anhui University, Hefei, China. His research interests include remote sensing image processing, technology, and applications of vegetation.

Dongyan Zhang received the Ph.D. degrees with major in agricultural remote sensing and information technology from Zhejiang University, Zhejiang, China, in 2012.

His research interests include computer image processing, hyperspectral remote sensing, and sensors applying in agriculture and environment.